smart cities

MDPI

Article

Intelligent Urban Flood Management Using Real-Time Forecasting, Multi-Objective Optimization, and Adaptive Pump Operation

Li-Chiu Chang [1,2], Ming-Ting Yang [3], Jia-Yi Liou [3], Pu-Yun Kow [3] and Fi-John Chang [3,*]

[1] Department of Water Resources and Environmental Engineering, Tamkang University, New Taipei City 25137, Taiwan; changlc@mail.tku.edu.tw
[2] Department of Artificial Intelligence, Tamkang University, New Taipei City 25137, Taiwan
[3] Department of Bioenvironmental Systems Engineering, National Taiwan University, Taipei 10617, Taiwan; r10622042@ntu.edu.tw (M.-T.Y.); r07622038@ntu.edu.tw (J.-Y.L.); steveyunkow@ntu.edu.tw (P.-Y.K.)
* Correspondence: changfj@ntu.edu.tw

Highlights

What are the main findings?

- The Intelligent Flood Control Decision Support System (IFCDSS) is an innovative AI framework integrating forecasting, optimization, and adaptive control for proactive urban flood management;
- The IFCDSS improved the pump operation efficiency by 45.4%, significantly outperforming the traditional flood control methods.

What are the implications of the main findings?

- The IFCDSS provides a robust, adaptable AI-driven solution optimizing flood mitigation, energy efficiency, and infrastructure resilience across diverse urban contexts;
- It represents a significant advancement toward autonomous flood management, integrating early warnings, intelligent decision support, and real-time optimization to protect lives, infrastructure, and ecosystems from escalating climate-induced flood risks.

Abstract: Climate-induced extreme rainfall events are increasing the intensity and frequency of flash floods, highlighting the urgent need for advanced flood management systems in climate-resilient cities. This study introduces an Intelligent Flood Control Decision Support System (IFCDSS), a novel AI-driven solution for real-time flood forecasting and automated pump operations. The IFCDSS integrates multiple advanced tools: machine learning for rapid short-term water level forecasting, NSGA-III for multi-objective optimization, the TOPSIS for robust multi-criteria decision-making, and the ANFIS for real-time pump control. Implemented in the flood-prone Zhongshan Pumping Station catchment in Taipei, the IFCDSS leveraged real-time sensor data to deliver accurate water level forecasts within five seconds for the next 10–30 min, enabling proactive and informed operational responses. Performance evaluations confirm the system's scientific soundness and practical utility. Specifically, the ANFIS achieved strong accuracy (R^2 = 0.81), with most of the prediction errors being limited to a single pump unit. While the conventional manual operations slightly outperformed the IFCDSS in minimizing flood peaks—due to their singular focus—the IFCDSS excelled in balancing multiple objectives: flood mitigation, energy efficiency, and operational reliability. By simultaneously addressing these dimensions, the IFCDSS provides a robust and adaptable framework for urban environments. This study highlights the transformative potential of intelligent flood control to enhance urban resilience and promote sustainable, climate-adaptive development.

check for updates

Academic Editor: Pierluigi Siano

Received: 17 April 2025
Revised: 27 May 2025
Accepted: 28 May 2025
Published: 29 May 2025

Citation: Chang, L.-C.; Yang, M.-T.; Liou, J.-Y.; Kow, P.-Y.; Chang, F.-J. Intelligent Urban Flood Management Using Real-Time Forecasting, Multi-Objective Optimization, and Adaptive Pump Operation. *Smart Cities* **2025**, *8*, 91. https://doi.org/10.3390/smartcities8030091

Keywords: artificial intelligence; urban drainage system; flood control; pump operation optimization; early warning; decision support; energy efficiency

1. Introduction

Urban flood management faces increasing challenges due to climate-change-induced extreme rainfall, urbanization, population growth, aging infrastructure, regulatory shifts, and environmental concerns [1–3]. Intense rainfall can overwhelm drainage systems, leading to severe societal, economic, and environmental consequences worldwide [4,5]. Densely populated estuarial cities like Taipei, Taiwan, are particularly vulnerable, as rapid urbanization and climate change already strain fragile drainage systems. Extreme weather events, fueled by global warming, frequently trigger flash floods that disrupt daily life, damage infrastructure, and hinder economic activities [6]. In flood-prone regions, rising sea levels and storm surges further exacerbate these risks. To address these challenges, climate-responsive, proactive, and integrated strategies are essential for ensuring urban sustainability and resilience [7,8]. Traditional flood management is reactive, relying on fragmented data that fail to intricately capture urban flood dynamics. Challenges include data scarcity, an uneven distribution of equipment, model limitations, and the absence of digital twins. Some models may overlook or insufficiently integrate real-time river and weather data, which can hinder their ability to accurately simulate scenarios and correct errors, potentially leading to reduced effectiveness over time. Effective flood management requires a comprehensive, data-driven approach that integrates diverse information sources—weather forecasts, sensor networks, and historical flood records—and a reliable pump operation system, critically enabling vulnerability assessments, accurate risk predictions, and proactive flood mitigation [9–12]. Despite the promising benefits of smart flood management systems [13–15], their widespread implementation remains limited. By leveraging data, technology, and advanced modeling, these systems can enhance decision-making, bolster infrastructure resilience, and safeguard communities from the unpredictable impacts of climate change. Effective stormwater management is crucial for protecting both built and natural environments.

Artificial intelligence (AI) technologies, such as machine learning, deep learning, and computer vision, along with remote sensing and environmental impact analyses, are revolutionizing flood management by advancing both the research and practical applications [16–18]. Ref. [19] proposed a metaheuristic-enhanced categorical boosting algorithm to improve flood-prone area mapping by documenting past flood events and providing historical insights for improved flood risk assessments. Ref. [20] offers a comprehensive analysis of the machine learning techniques used in flood susceptibility mapping. Integrating real-time sensor networks with AI enhances the forecasting accuracy by leveraging historical, topographical, and environmental data to uncover insights often missed by the conventional models. AI-powered early warning systems provide real-time analyses and timely alerts, improving community preparedness. For example, ref. [21] found that predictive real-time control strategies are more effective than reactive approaches in managing urban stormwater storage. These advancements are crucial for strengthening urban resilience and sustainability, aligning flood management with broader efforts to enhance livability and protect vulnerable areas [11,22].

AI transforms urban flood management by efficiently processing complex datasets—including satellite imagery, meteorological inputs, and terrain information—to significantly enhance the accuracy of flood predictions. By learning from historical flood patterns and integrating real-time IoT data, AI facilitates rapid forecasting and the development of digital twins. Crucially, AI enables automated pumping station operations by employing predictive analytics and adaptive control algorithms, dynamically optimizing pump activation decisions. This capability markedly improves operational responsiveness, the effectiveness of flood mitigation, and infrastructure resilience compared to the conventional manual approaches. Key AI methods employed include machine learning models for accurate inundation forecasting, NSGA-based algorithms for multi-objective optimization of automated pumping station operations, the ANFIS for real-time adaptive control over pumping systems, and the Technique for Order Preference by Similarity to Ideal Solution (TOPSIS) for robust multi-criteria decision analyses. These methods are crucial for enhancing the automation and effectiveness of flood defenses amid escalating climate risks. Machine learning has consistently demonstrated efficacy in flood forecasting and optimization [23–26]. NSGAs have been extensively utilized in water resource management [27–33], and the TOPSIS is widely adopted across diverse engineering applications [34–37]. The ANFIS, integrating fuzzy logic and neural networks, has effectively supported reservoir safety forecasting and flood impact assessments [38–41]. Collectively, these AI-driven tools significantly strengthen urban flood resilience, optimize the operational strategies, and advance sustainable water management. Nevertheless, challenges related to data availability, the computational demands, and real-time integration within dynamic urban environments remain critical for their practical implementation.

Taipei City, located in a low-lying basin surrounded by mountains and intersected by the Keelung and Tamsui Rivers, is highly susceptible to flooding due to its geographic and climatic conditions. This city frequently experiences short-duration, high-intensity rainfall events, including thunderstorms and typhoon-induced downpours that can overwhelm drainage systems. Despite advancements such as IoT-based monitoring and pump station operations, challenges persist, particularly in low-lying areas below high tide levels. Events like Typhoon Soudelor in 2015 highlight the limitations of the current infrastructure and the growing need for integrated, data-driven flood management strategies.

To address these challenges, this study aims to develop a comprehensive smart city flood warning and automated pump operation system. This system will establish forecasting models for the water levels in sewers, optimize pumping station operations, deliver flood forecasts within 5 s for the next 10 to 30 min, and present real-time forecast results to aid disaster response decision-making. We introduce the Intelligent Flood Control Decision Support System (IFCDSS) to bridge the gap between AI-driven flood forecasting and real-time operational management. The IFCDSS integrates real-time sensor data, AI-powered predictive analytics, and adaptive decision-making frameworks to enhance the effectiveness of flood responses. This approach ensures that AI applications in urban flood management are not only predictive but also actionable, scalable, and responsive to evolving climate challenges. The system follows a three-stage framework: real-time data integration, AI-powered emergency response analyses, and adaptive learning via neural networks. It incorporates a hybrid CNN-BP model for water level forecasting, NSGA-III for multi-objective optimization, the ANFIS for adaptive pumping strategies, and the TOPSIS for multi-criteria decision-making, enabling efficient flood mitigation. Focused on Taipei's Zhongshan Pumping Station catchment, the IFCDSS provides early warnings, inundation mapping, and optimized pumping station operations to minimize flood hazards. By combining real-time monitoring, advanced forecasting, and AI-driven decision-making tools, the system enhances disaster resilience, reduces infrastructure damage, and offers a scalable, data-driven solution to the challenges of climate-induced flooding.

2. Materials and Methods

2.1. The Study Area

Taipei City, the capital and economic hub of Taiwan, is highly vulnerable to urban flooding due to its geographic and hydroclimatic characteristics. Located within the Taipei Basin, the city is bordered by mountains on three sides, with the Keelung River flowing through its center and the Tamsui River flowing to the north. Its low-lying terrain, coupled with orographic effects, exacerbates flood risks, especially during typhoon seasons and summer thunderstorms that deliver intense, short-duration rainfall capable of overwhelming drainage systems. With an average annual rainfall of 2405 mm, 36% of which occurs during typhoon seasons, Taipei faces significant flooding challenges, particularly in low-lying areas along rivers, some of which are below the average high tide levels. These areas require robust flood defenses to mitigate the impacts of extreme weather events.

To address these challenges, Taipei has developed world-class flood management infrastructure, including an advanced network of underground sewers and strategically placed pumping stations designed to protect the city's 2.5 million residents. This system is enhanced further by a comprehensive IoT network that monitors rainfall, sewer flows, stream levels, and pumping station operations in real time. The pumping stations, located at the endpoints of the sewer system, play a crucial role in extracting and discharging water. Under normal conditions, the gravity gates remain open, allowing rainwater to flow naturally into rivers. During typhoons or heavy rainfall, the pumps are activated to discharge excess water rapidly, preventing water accumulation and mitigating the risk of urban flooding.

This study focuses on the Zhongshan Pumping Station catchment area in southwestern Taipei within the Keelung River Basin, as shown in Figure 1a. Covering approximately 481 hectares, this low-lying region faces significant drainage challenges. The Zhongshan Pumping Station, situated downstream, is supported by an extensive monitoring network that includes five rain gauge stations and seven sewer water level gauge stations, providing accurate data to inform flood control strategies. The dataset used in this research, provided by the Taipei City Government's Hydraulic Engineering Office, spans from 2006 to 2021 and includes rainfall, sewer water levels, internal (forebay) and external (river) water levels, and pump operations. Rainfall in Taipei follows distinct seasonal patterns: spring rains (February–April), plum rains (May–June), and intense storms or typhoons (July–September). The dataset, processed at 10 min intervals with event segmentation and imputation, includes 230 rainfall events recorded across four rain gauge stations and 132 pump operation events, yielding a total of 9670 data points. Figure 1b illustrates the facilities of the Zhongshan Pumping Station, which is equipped with nine vertical shaft pumps (seven at Site 1 and two at Site 2), with a combined capacity of 79 cubic meters per second (cms). The station primarily operates based on rainfall and water levels. Historical records show that 85% of operations involved activating one to three pumps, providing valuable insights into the operational responses and flood control strategies essential for effective urban flood management.

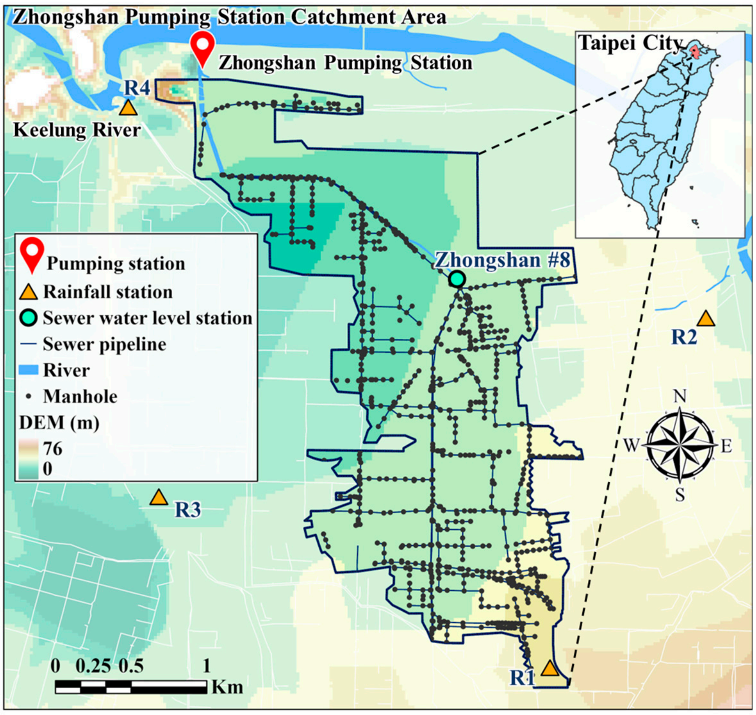

(**a**)

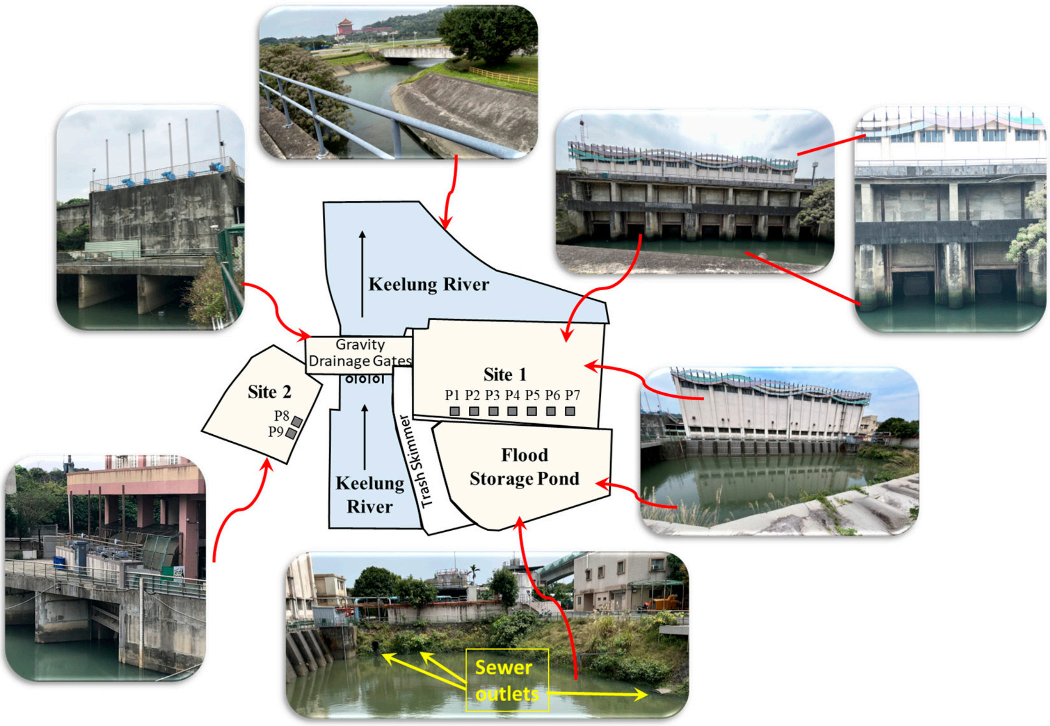

(**b**)

Figure 1. Illustrations of the study area. (**a**) Location of Zhongshan Pumping Station. (**b**) Zhongshan Pumping Station.

2.2. Methodology

This study introduces an Intelligent Flood Control Decision Support System (IFCDSS), aiming to substantially enhance urban flood management and water resource sustainability (Figure 2). By leveraging data from IoT sensors, meteorological observations, and historical flood records, the IFCDSS generates actionable insights for precise flood responses and optimized pumping station operations, significantly improving the resilience to extreme weather events. The Zhongshan Pumping Station catchment area in Taipei City serves as the focal study region, where an integrated AI-driven approach is deployed.

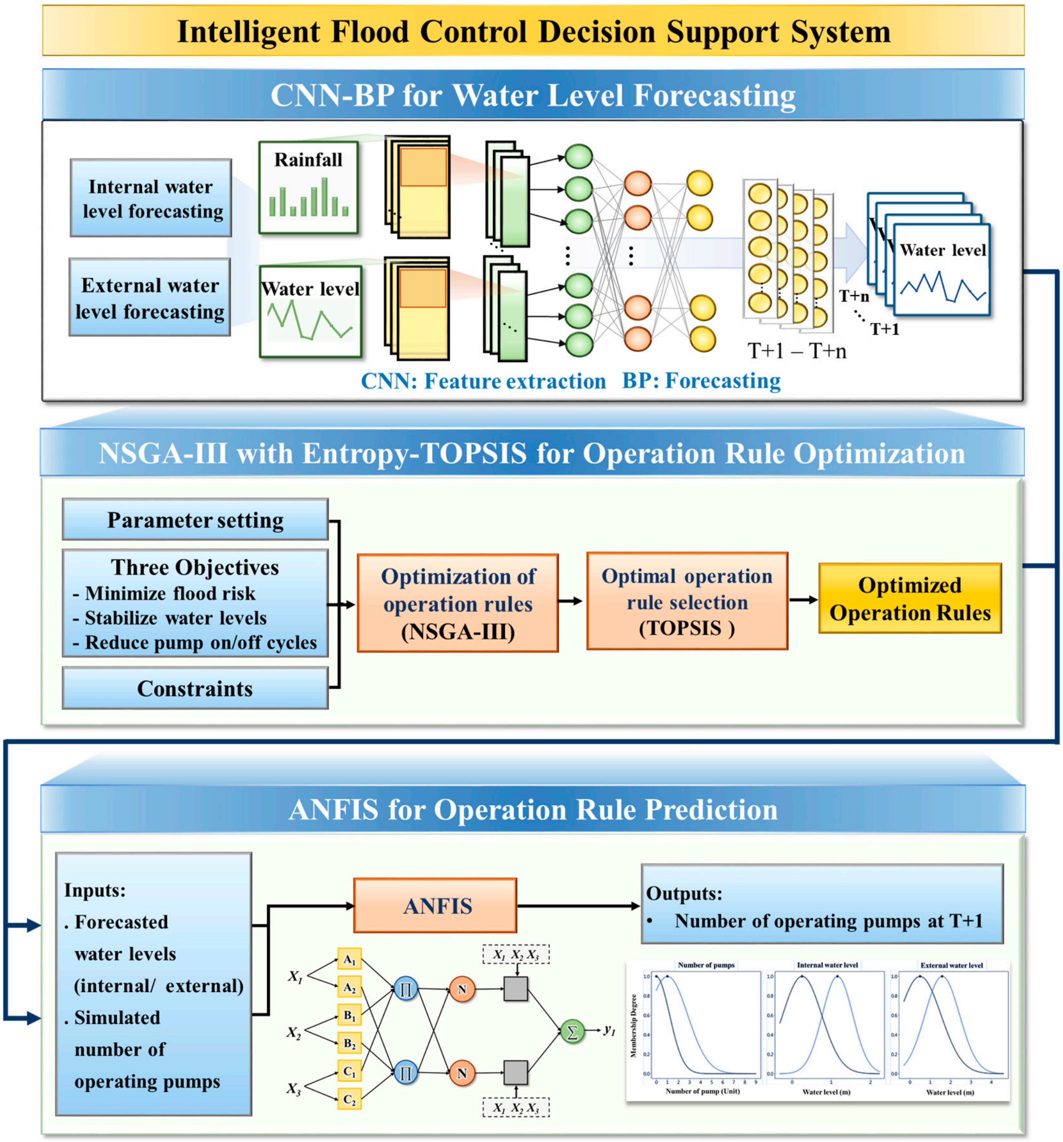

Figure 2. Research framework.

The key methodologies utilized and their justifications include the following:

- The CNN-BP model: A hybrid machine learning model combining a Convolutional Neural Network (CNN) and a Back Propagation Neural Network (BP), selected for its ability to effectively capture temporal–spatial correlations and achieve high-accuracy, multi-step water level forecasts.
- The NSGA-III algorithm: This was chosen for its capability to efficiently address complex multi-objective optimization problems, simultaneously minimizing flood hazards, stabilizing water levels, and reducing the pump switching frequency, thus ensuring robust operational strategies during flood events.
- The TOPSIS method: This was employed to systematically select the optimal pumping strategy from multiple NSGA-III-generated solutions. This approach objectively balances competing criteria, validated by comprehensive simulation comparisons with the historical and current operational guidelines.

- The ANFIS model: This was implemented for its strengths in integrating fuzzy logic with neural networks, effectively translating the simulated optimization results into accurate, real-time pump activation forecasts. Its adaptive nature ensures dynamic responsiveness under rapidly changing flood conditions.

By integrating these advanced forecasting, optimization, and adaptive decision-making methods, this comprehensive approach substantially enhances pumping station efficiency and operational resilience. The IFCDSS thus significantly advances autonomous urban flood management capabilities, providing scientifically rigorous support for sustainable water resource practices. The following sections provide detailed discussions of each methodological component.

2.2.1. The Hybrid Convolutional Neural Network and Backpropagation Neural Network (CNN-BP) Model

The hybrid CNN-BP model enhances urban drainage forecasting by integrating spatial–temporal features. The CNN captures the spatial dependencies among rainfall, sewer levels, and pump conditions, while the BPNN with chaotic neurons improves real-time classification and time-delay handling for accurate flood responses. This approach ensures precise short-term water level forecasts (10–60 min) across sewer, internal (forebay), and external (river) water contexts. For related methods and results, see [42].

2.2.2. Non-Dominated Sorting Genetic Algorithm III (NSGA-III)

This study employs NSGA-III to optimize pumping station operations, addressing multi-objective complexities in urban flood management. While a genetic algorithm (GA) can handle single-objective problems, ref. [43] introduced NSGA-II for multi-objective optimization, integrating non-dominated sorting, crowding-distance comparisons, and an elitist preservation strategy. However, NSGA-II struggles with many-objective problems due to its reduced convergence and diversity. To overcome this, ref. [44] developed NSGA-III, replacing the crowding-distance comparison with a niche preservation operation, using well-distributed reference points to enhance the diversity and convergence. By aligning solutions with these reference points, NSGA-III prevents crowding and uneven distributions, making it effective for complex, many-objective problems, such as environmental planning and flood management [45–49]. Overall, NSGA-III extends evolutionary algorithms' capabilities, ensuring a scalable performance for high-dimensional optimization challenges.

This study employs NSGA-III to optimize the pumping station's operational strategy, addressing the complexities of multi-objective decision-making in urban flood management. The following describes the model's objective functions, constraints, and parameter settings, followed by a comparative analysis with the current pumping station operation rules. NSGA-III's parameters (Table 1) include a real-number encoding scheme with 18 variables: 9 for the activation water levels and 9 for the deactivation water levels of pumps. The optimization runs 1000 iterations, applying selection, crossover, and mutation to refine the operation rules. Using the initial water levels, inflows, and new operational strategies, the model simulates the outflows, internal water levels, and Zhongshan #8's sewer water levels at the next time interval. The water level trajectories and the operation records for training events are simulated to calculate the objective functions and constraints, thereby evaluating the chromosome quality. Better chromosomes are retained and passed on to the next generation through non-dominated sorting and niche-preservation mechanisms.

Table 1. Parameter settings of NSGA-III.

Parameter Type	Parameter Setting/Method
Encoding method	Real-number
Number of chromosomes	18
Population size	1000
Number of objective functions	3
Number of constraints	4
Number of iterations	1000
Selection method	Tournament selection
Crossover method	Simulated binary crossover, probability: 80%
Mutation method	Polynomial mutation, probability: 5%

- Objectives

This multi-objective approach integrates operational stability, hazard mitigation, and resource efficiency to enhance pumping station performance under extreme weather conditions. Three objectives are delineated as follows.

Minimizing flood hazards (Obj_1):

This objective minimizes the sum of hazards, which is evaluated using Zhongshan #8's sewer water levels and internal water levels. The rules keep the water levels well below critical water levels during storms to reduce flood hazards. They reduce flood hazards by minimizing the maximum internal water level during events, ensuring a sufficient capacity for the inflow of sewer water, which directly impacts flood prevention. The calculation formulas are shown in Equations (1)–(3).

$$min(Obj_1) = 0.6 \times \sum_{j=1}^{J} \frac{\sum_{i=1}^{I} Range(sewer8_{j,i})}{length\ of\ j\ event} + 0.4 \times \sum_{j=1}^{J} Range(max\ (wl_j)) \tag{1}$$

$$Range(sewer8_{j,i}) = \begin{cases} 0, & \text{if } sewer8j, i < 0.81 \text{ m} \\ 2.056sewer8_{j,i}{}^2 - 2.954sewer8_{j,i} + 2.043, & \text{else} \end{cases} \tag{2}$$

$$Range(max\ (wl_j)) = \begin{cases} 0, & \text{if } smax\ (wl_j) < 1.02 \text{ m} \\ 3.636max\ (wl_j) + 1.709, & \text{else} \end{cases} \tag{3}$$

where j represents the j-th event, and i represents the i-th data within the event. $Range(sewer8_{j,i})$ denotes the hazard value of Zhongshan #8's sewer water level (m) at the i-th data point in the j-th event. $Range(max(wl_j))$ represents the hazard value of the maximum internal water level (m) during the j-th event, and the length of the j-th event refers to the total data length of the event. $sewer8_{j,i}$ denotes Zhongshan #8's sewer water level (m) at the i-th data point in the j-th event. $max\ (wl_j)$ denotes the maximum internal water level (m) during the j-th event.

Minimizing variability in the water level (Obj_2):

This objective promotes stability in the internal water levels to reduce the frequency of pump activation. Lower fluctuations in internal water levels result in reduced pump switching, improving the operational efficiency and reducing pump wear. The calculation formula is shown in Equation (4).

$$min(Obj_2) = \sum_{j=1}^{J} \sum_{i=2}^{I} |wl_{j,i} - wl_{j,i-1}| \tag{4}$$

where j represents the j-th event, i represents the i-th data point within the event, and $wl_{j,i}$ denotes the internal water level (m) at the i-th data point during the j-th event.

Minimizing the pump switching frequency (Obj_3):

This objective limits frequent activation of the pump to decrease its energy consumption, maintenance costs, and wear while maintaining effective flood control. The average number of pump activation cycles is calculated per event to assess the operation performance. Lowering the number of active pumps while effectively controlling the internal water level would reduce the energy consumption and power costs. Smart operational rules minimize on–off cycling and operate the pumps during off-peak hours when possible. The calculation formula is shown in Equation (5).

$$min(Obj_3) = \frac{\sum_{j=1}^{J} \sum_{i=2}^{I} \left| pump_{j,i} - pump_{j,i-1} \right|}{length\ of\ all\ events} \quad (5)$$

where j represents the j-th event, i represents the i-th data point within the event, $pump_{j,i}$ denotes the number of pumps in operation at the i-th data point during the j-th event, and *length of all events* refers to the total data length of all events.

- Constraints

To ensure that the pump operation results are practical, the constraints are divided into pump constraints and actual operation constraints. These constraints are formulated as follows.

Number of operating pumps:

At any moment, the number of active pumps cannot exceed the actual number of pumps available, as shown in Equation (6).

$$0 \le PN_{j,i} \le PN_{max} \quad (6)$$

where $PN_{j,i}$ represents the number of pumps in operation at the i-th data point during the j-th event, and PN_{max} refers to the maximum number of pumps.

Operating water level:

Each type of pump has a minimum operating water level, which limits the water level at which the pumps can be activated, as shown in Equations (7)–(9).

$$0.5\text{ m} \le WL_k \le 2.78\text{ m}, \quad k = \#1 - \#2\ (\text{Site1}) \quad (7)$$

$$1.3\text{ m} \le WL_k \le 2.78\text{ m}, \quad k = \#3 - \#7\ (\text{Site1}) \quad (8)$$

$$1.3\text{ m} \le WL_k \le 2.78\text{ m}, \quad k = \#8 - \#9\ (\text{Site2}) \quad (9)$$

where WL_k is the internal water level (m) for the k-th pump.

Sequential pump activation:

Pump activation depends on the internal water level. An increase in inflow raises the internal water level, which may require activating additional pumps. There is a positive correlation between the internal water level and the number of active pumps. Pump activation should follow a predefined sequence corresponding to the internal water level, as shown in Equations (10) and (11).

$$PAL_q < PAL_{q+1}, \quad q = \#1 - \#9 \quad (10)$$

$$PAN_q < PAN_{q+1}, \quad q = \#1 - \#9 \quad (11)$$

where PAL_q is the water level for pump activation (m) for the q-th pump activated, and PAN_q is the number of activations for the q-th pump activated.

Sequential pump deactivation:

Pump deactivation is also related to the internal water level. Pumps should be deactivated in sequence based on the internal water level. The activation water level must be higher than the deactivation level to ensure a smooth operation process, as shown in Equations (12) and (13).

$$PDL_q < PDL_{q+1}, \quad q = \#1 - \#9 \tag{12}$$

$$PDN_q < PDN_{q+1}, \quad q = \#1 - \#9 \tag{13}$$

where PDL_q is the pump deactivation water level (m) for the q-th pump deactivated, and PDN_q is the number of deactivations for the q-th pump deactivated.

2.2.3. Technique for Order Preference by Similarity to Ideal Solution (TOPSIS)

The TOPSIS, developed by [50], is a widely used multi-criteria decision analysis method. It identifies the solutions closest to the ideal outcome and farthest from the worst-case scenario, ensuring a balanced evaluation. This process includes normalization, distance calculation, and ranking of the alternatives based on their relative closeness to the ideal solution. Known for its computational efficiency and adaptability to both qualitative and quantitative criteria, the TOPSIS is extensively applied in resource management [51,52] and environmental planning [53]. This study adopts the TOPSIS to select the best solution from a suite of NSGA-III Pareto solutions.

2.2.4. The Adaptive-Network-Based Fuzzy Inference System (ANFIS)

The ANFIS, proposed by [54], combines the strengths of fuzzy logic and neural networks to overcome their respective limitations. While fuzzy logic effectively handles uncertainty and imprecision through IF-THEN rules, it lacks self-learning capabilities. Conversely, neural networks excel at learning from data but lack transparency in human-like reasoning. The ANFIS integrates these approaches, combining a fuzzy inference system (FIS) with the supervised learning of a feedforward neural network to achieve both adaptability and interpretability. For real-time pump operations, the ANFIS constructs a predictive model that determines the optimal number of pumps to activate based on NSGA-III's optimized operational results. By continuously adjusting the pumping strategies in response to changing conditions, the ANFIS enhances the system's adaptability and efficiency, ensuring precise and proactive flood management.

3. Results and Discussion

This section presents the outcomes of the proposed IFCDSS, focusing on three core components: water level forecasting, optimization of pumping station operations, and the integration of predictive modeling with adaptive decision-making. The operational strategies were optimized using NSGA-III, and the number of pumps required under different scenarios was predicted using the ANFIS, informed by real-time water level forecasts and operational rules.

3.1. Water Level Forecasts

In this study, the CNN-BP model was employed for water level forecasting. A brief introduction of the input parameters and hyperparameter settings is given in the Supplementary Material. The hybrid CNN-BP model demonstrated high accuracy in generating multi-input, multi-output, and multi-step forecasts for urban stormwater systems. Forecasts were made for the sewer water levels (10–40 min ahead) as well as the internal (forebay) and external (river) water levels at the Zhongshan Pumping Station (10–60 min ahead) at 10 min intervals. At a short-term forecast horizon (T + 1), the model achieved a root mean square error (RMSE) of 0.08 m for sewer water levels and 0.06 m for both internal and external water levels, indicating a strong forecasting performance. These results validate the model's robustness and reliability in capturing the dynamic and nonlinear behavior of urban drainage systems under varying hydro-climatic conditions.

The model's performance is attributed to the effective combination of the CNN for spatial pattern recognition and the BPNN for temporal sequence learning. The high forecasting accuracy supports its integration into real-time flood management systems, facilitating proactive decision-making. For further methodological details and an expanded performance analysis, refer to [42].

3.2. The Optimization of Pumping Station Operations

Traditional pumping station operations often depend on operators' experience and heuristic decision-making, which can lead to suboptimal outcomes, especially during high-intensity storm events. To improve its operational efficiency and reliability, this study employed NSGA-III to optimize the control strategies for a nine-pump system. The model encoded 18 decision variables, representing the activation and deactivation thresholds for the pumps, and simultaneously optimized three conflicting objectives:

- Obj_1: Minimize continuous flood hazard values;
- Obj_2: Reduce the difference in water levels across the pump system;
- Obj_3: Limit the frequency of pump switching.

An initial population was constructed using a 90:10 ratio of randomly generated to manually designed chromosomes, ensuring both diversity and domain relevance for effective convergence. Simulations were conducted using the projected internal and sewer water levels under various inflow conditions. The dataset included 24 training events (2120 data points) and 14 testing events (659 data points), derived from historical inflow records. Optimized rules derived from the training events were applied to testing events, and the results were evaluated using the three objective functions under system constraints.

After 1000 iterations, NSGA-III produced 255 non-dominated solutions, demonstrating an effective balance among the competing objectives. The outcomes were analyzed in a 3D objective space (Figure 3), with the key observations summarized below:

- Obj_1 vs. Obj_2 (XY view—flood hazard vs. water level difference): A slightly negative correlation was observed, with most of the solutions concentrated within the 97–99 m range for Obj_2. However, the limited spread of Obj_2 values implies that further reductions in the internal water level yield diminishing returns in terms of overall flood hazard mitigation. This suggests that while differences in water levels have some influence on minimizing flood hazards, their marginal impact becomes less significant once the difference is already within an operational band (97–99 m).
- Obj_1 vs. Obj_3 (XZ view—flood hazard vs. pump switching frequency): A clear negative correlation was evident. This indicates that achieving fewer flood hazards generally required more frequent pump operations. This trade-off is primarily influenced by fluctuations in internal water levels and variations in Zhongshan #8's sewer water level, which necessitate timely pump activation to prevent water accumulation. As a result, strategies that are effective in mitigating flood hazards tend to involve higher pump responsiveness, leading to an increase in switching frequency.
- Obj_2 vs. Obj_3 (YZ view—water level difference vs. pump switching frequency): A positive correlation was observed, indicating that higher differences in water levels led to increased pump switching. This suggests that larger fluctuations in water levels tend to trigger more frequent pump activations. As pump switching becomes more frequent,

it introduces greater variability into both the internal water levels and system outflows, potentially leading to less stable operations.

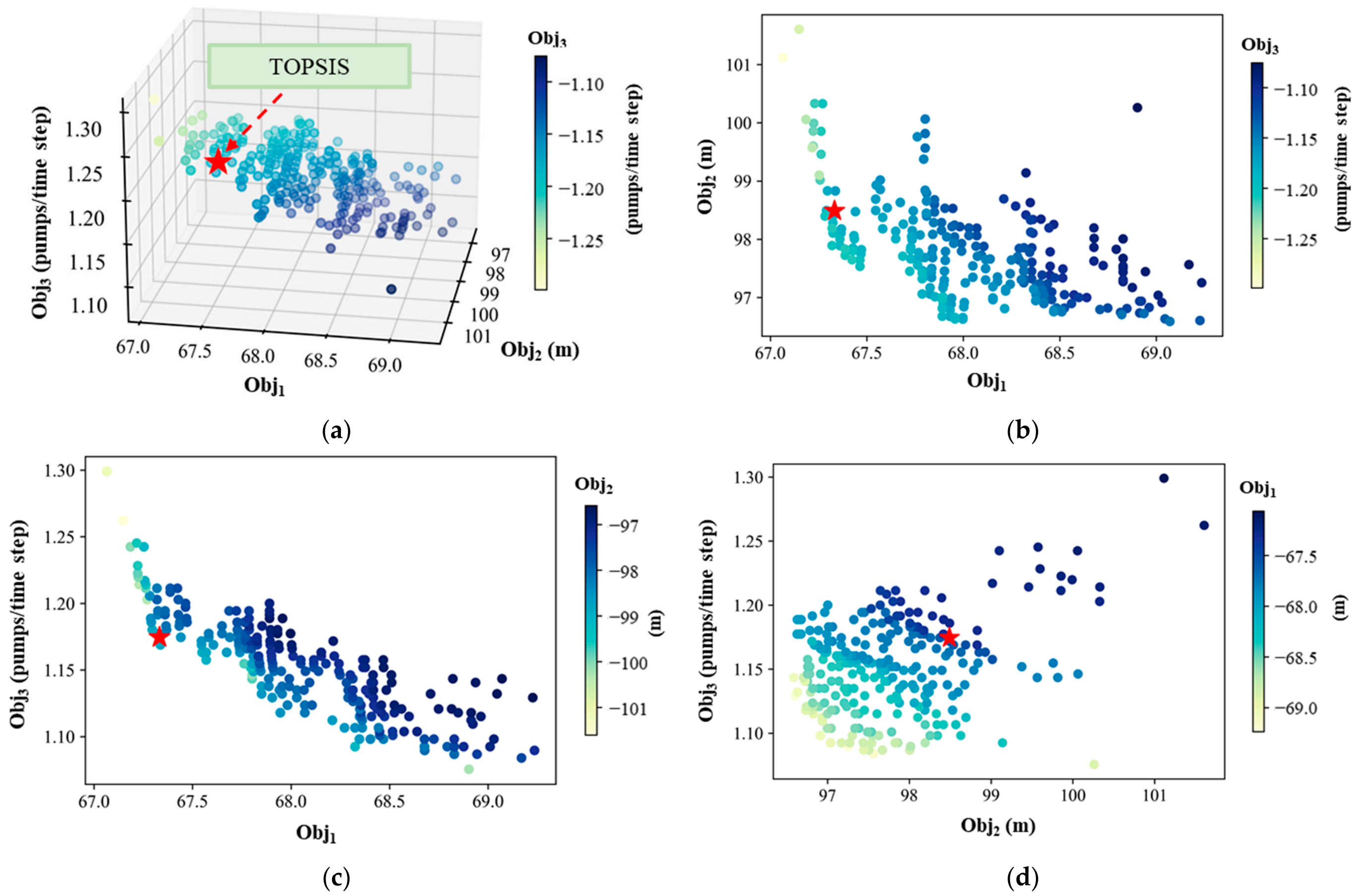

Figure 3. Pareto front of 255 converged solutions obtained from NSGA-III. (**a**) Pareto front. (**b**) Obj_1 vs. Obj_2. (**c**) Obj_1 vs. Obj_3. (**d**) Obj_2 vs. Obj_3. The asterisk shown in (**b**,**d**) denotes the optimal solutions selected by the TOPSIS. Obj_1 optimizes flood hazards. Obj_2 stabilizes internal (forebay) water levels. Obj_3 reduces pump switching frequency.

Overall, the results highlight key trade-offs in pumping station management: efforts to minimize flood hazards (Obj_1) often necessitate more frequent pump activation (Obj_3) and may inadvertently increase variability in the water levels (Obj_2). These insights underscore the value of multi-objective optimization frameworks, like NSGA-III, in developing robust, adaptive, and balanced operational strategies for urban flood control.

3.3. TOPSIS-Based Solution Selection

In refining the NSGA-III optimization outcomes, the TOPSIS was employed to prioritize flood hazard reductions (Obj_1). Among the 255 non-dominated solutions, the top 10% (26 solutions) with the lowest flood hazard values were shortlisted as finalists, marked with asterisks in Figure 3. The objective function values are detailed in Table 2.

Table 2. Values of the objective functions of the optimal solution selected by the TOPSIS.

Objective	Value		
	Obj_1	**Obj_2 (m)**	**Obj_3 (Pumps/Time Step)**
Obj_1 (Minimizing flood hazards)	67.07	101.11	1.30
Obj_2 (Minimizing water level difference)	69.07	96.59	1.14
Obj_3 (Minimizing pump switching frequency)	68.90	100.26	1.08

Using the TOPSIS, the best solution was identified, achieving optimal trade-offs among the objectives by maximizing the proximity to the ideal solution while minimizing deviations. The optimized pump operation rules, illustrated in Figure 4, significantly outperform the traditional strategies, emphasizing enhanced flood hazard management.

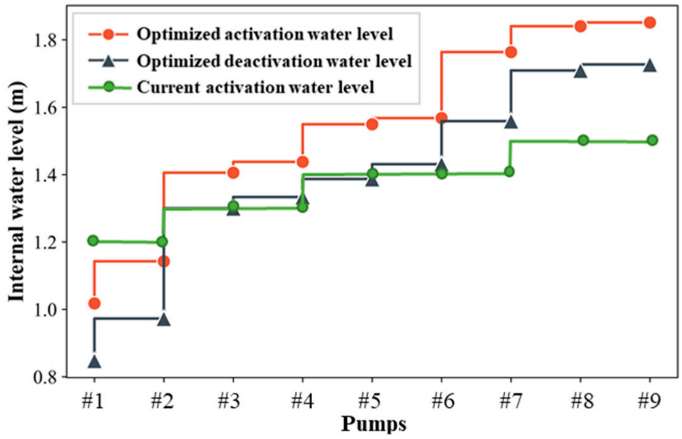

Figure 4. Optimal operation rules selected by the TOPSIS from the NSGA-III Pareto front.

Key adjustments in the selected rule set include the following:

- Lower activation thresholds than the current ones for the first and second pumps, which increase the storage capacity available in the initial stages of a rainfall event, thereby enhancing early flood mitigation;
- Higher activation thresholds than the current ones for the third to ninth pumps, which increase the operational efficiency and reduce energy use, in alignment with the NSGA-III optimization outputs;
- Stable thresholds for the third to sixth pumps, maintaining consistency and operational reliability in moderate rainfall conditions;
- High thresholds for the seventh to ninth pumps, optimizing the energy use and response timing during peak flow scenarios.

These tailored adjustments effectively balance flood hazard reductions with operational efficiency, offering a resilient and adaptive framework for managing pumping station operations during extreme weather events. The integration of the TOPSIS ensures that the final decision reflects a holistic evaluation of competing objectives, enabling more informed and justifiable operational strategies under uncertainty.

3.4. Evaluation of the Optimized Operational Rules

The simulation results based on the TOPSIS-selected optimized operational rules obtained from NSGA-III revealed significant enhancements in the pumping station performance across multiple objectives compared to the current operation rules (Figure 5). Specifically, the optimized rules for reducing water level differences (Obj_2) achieved a 50.51% improvement during the training phase and a 45.4% improvement during the testing phase compared to the baseline (current) operational strategies.

In terms of the pump switching frequency (Obj_3), the optimized operations significantly reduced excessive pump activation, showing an 82% improvement in the training phase and a 28% improvement in the testing phase. While manual operations marginally outperformed the optimized strategies in minimizing flood hazards (Obj_1), this outcome reflected the focus of manual operations solely on flood hazard reductions. In contrast, the AI-driven rules provided a more balanced and consistent trade-off among competing objectives, underscoring the importance of multi-objective optimization in addressing complex urban flood control scenarios.

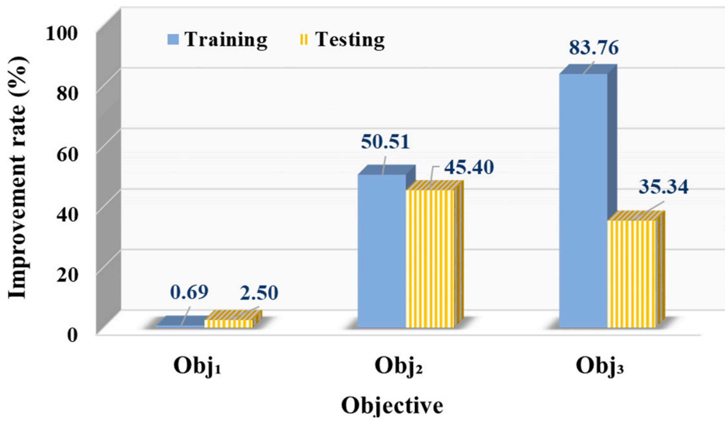

Figure 5. The improvement rate of the TOPSIS-selected optimized operation rules obtained from NSGA-III over the current operation rules for three objectives. Obj_1 optimizes flood hazards. Obj_2 stabilizes internal (forebay) water levels. Obj_3 reduces the pump switching frequency.

These findings highlight the potential of AI-based approaches to enhance the operational efficiency and automation of flood management systems, not only outperforming the current rule-based operations but also complementing human expertise with data-driven precision.

Performance Evaluation for Typhoon and Heavy Rainfall Events

To validate the system's robustness further, the TOPSIS-selected optimized rules were evaluated against two real flood events: Typhoon Mitag (2019) and a heavy rainfall event on 4 June 2021.

- Typhoon Mitag (2019):

During this event, the optimized rules initiated earlier and less frequent pump activations, effectively reducing internal water levels during the recession phase (Figure 6a). Despite the overestimation of water levels due to the exclusion of gravity drainage dynamics, the optimized strategy maintained greater stability and resulted in a lower final water level compared to that in the current operation (Figure 6b).

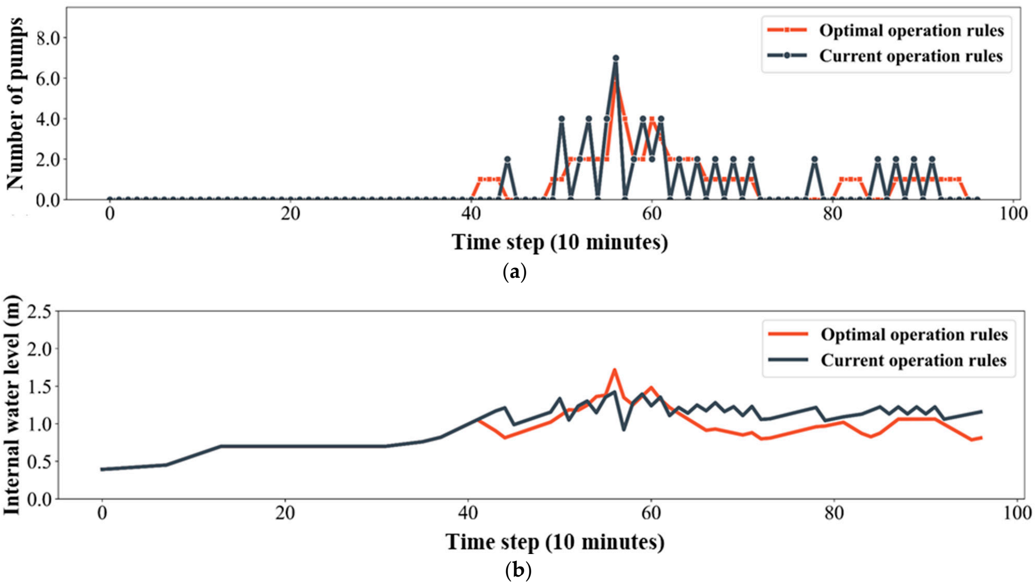

Figure 6. A comparison of the operational results based on the TOPSIS-selected optimal operation rules obtained from NSGA-III and the current operation rules for Typhoon Mitag, 2019. (**a**) The number of operating pumps. (**b**) The number of operating pumps.

- Heavy rainfall on 4 June 2021:

In this case, the optimized rules slightly overestimated the peak inflows, again due to the unmodeled gravity drainage dynamics. Nevertheless, they proved more efficient during the recession phase, reducing both the pump activation frequency and the variability in water levels. While a slightly higher peak water level was observed, the optimized strategy effectively smoothed the system's response and minimized unnecessary pump activity (Figure 7a,b).

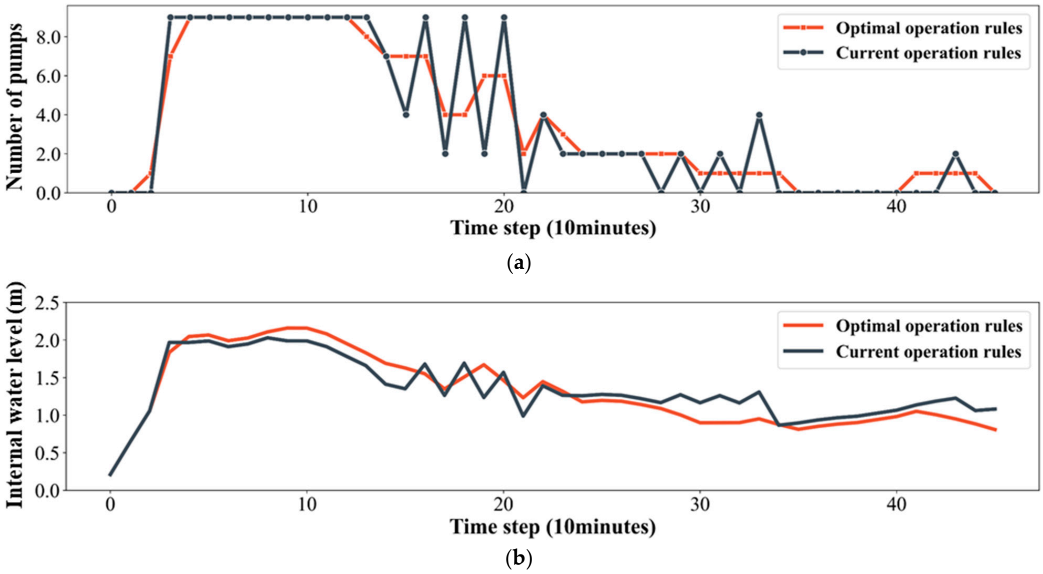

Figure 7. A comparison of the operational results based on the TOPSIS-selected optimal operation rules obtained from NSGA-III and the current operation rules for a heavy rainfall event on 4 June 2021. (**a**) The number of operating pumps. (**b**) The number of operating pumps.

Across both events, the NSGA-III-optimized rules successfully balanced water level control and pump efficiency, reducing the pump switching frequency, mitigating water level fluctuations, and helping to minimize pump wear and tear. While experienced operators can sometimes outperform automated systems under specific conditions, the proposed optimization framework provides a reliable, scalable foundation for future automated, real-time pumping station management, contributing to improved flood resilience and urban infrastructure sustainability.

3.5. Integration of the Water Level Forecasts and Operational Strategies for Early Warnings

To enhance the operational responsiveness, this study integrated internal and external water level forecasts with the TOPSIS-selected optimized operational rules obtained from NSGA-III as inputs into the ANFIS. By leveraging fuzzy logic to simulate human decision-making, the ANFIS model predicts the number of pumps required in the next 10 min (T + 1), offering early operational recommendations. This integration provides a more intelligent and anticipatory approach to autonomous pumping management under dynamic flood conditions.

3.5.1. The Dataset and Model Inputs

The same flood events used for NSGA-III optimization were employed and partitioned into training (16 events, 1487 records), validation (9 events, 440 records), testing (8 events, 454 records), and additional testing (5 events, 370 records) datasets. Table 3 presents the statistical indices of flood events for constructing the ANFIS model. It is noted that no significant differences were observed across the datasets in terms of water levels or pump operations, aside from a slightly higher maximum external water level in the training dataset.

Table 3. A summary of the statistical indices of flood events for constructing the ANFIS model across modeling phases.

Item	Phase	Maximum	Minimum	Mean	Standard Deviation
Number of pumps	Training	9.00	0.00	1.17	2.04
	Validation	9.00	0.00	1.09	1.61
	Testing	9.00	0.00	0.80	1.44
	Additional testing	9.00	0.00	0.86	1.59
Internal water level (m)	Training	3.71	0.01	1.11	0.57
	Validation	2.94	0.02	1.06	0.48
	Testing	2.91	0.00	0.97	0.48
	Additional testing	2.98	0.00	0.99	0.51
External water level (m)	Training	4.80	−0.28	1.50	0.84
	Validation	2.85	0.05	1.56	0.64
	Testing	2.60	−0.22	1.20	0.66
	Additional testing	2.64	0.03	1.29	0.75

The input variables were selected based on a correlation analysis, targeting the internal (forebay) water levels (T − 1 to T + 2), external (river) water levels (three moderately correlated time steps (T to T + 2)), and pump operation data (four highly autocorrelated time steps (T to T − 3)). The model was trained using subtractive clustering, with an influence radius of 0.5 and a squash factor of 1.25, optimizing the fuzzy inference structure for accurate simulation of operational decision-making.

3.5.2. The Model Performance

Compared to the simulated results of the TOPSIS-selected optimized operational rules obtained from NSGA-III, the ANFIS model exhibited a strong predictive performance, achieving an overall R^2 of 0.81 between the predicted and simulated pump activation counts. Most of the prediction errors fell within one pump, indicating reliable tracking of operational trends.

Figure 8 presents the predicted and simulated results for additional testing phases, including a time series comparison of the simulated vs. predicted pump activations (Figure 8a), internal water level fluctuations (Figure 8b), and the differences between the simulated and predicted numbers of pumps activated (Figure 8c). While the ANFIS model accurately captured the overall trends, the prediction errors increased during periods of rapid changes in water levels. Specifically, underestimations occurred during sharp rises in water levels (e.g., time steps of 56–63, 226–237, and 258–262), reflecting a delayed model response, whereas overestimations emerged during rapid declines in water levels or abrupt changes from the previous levels, again suggesting a lag in adaptation.

These limitations are likely due to the training data being skewed toward low-pump-activation scenarios, limiting the model's capacity to learn complex patterns associated with high-flow events. Despite this, the model performed well under conditions of moderate variability in water levels and low to medium pump activation, supporting its applicability in typical operational contexts.

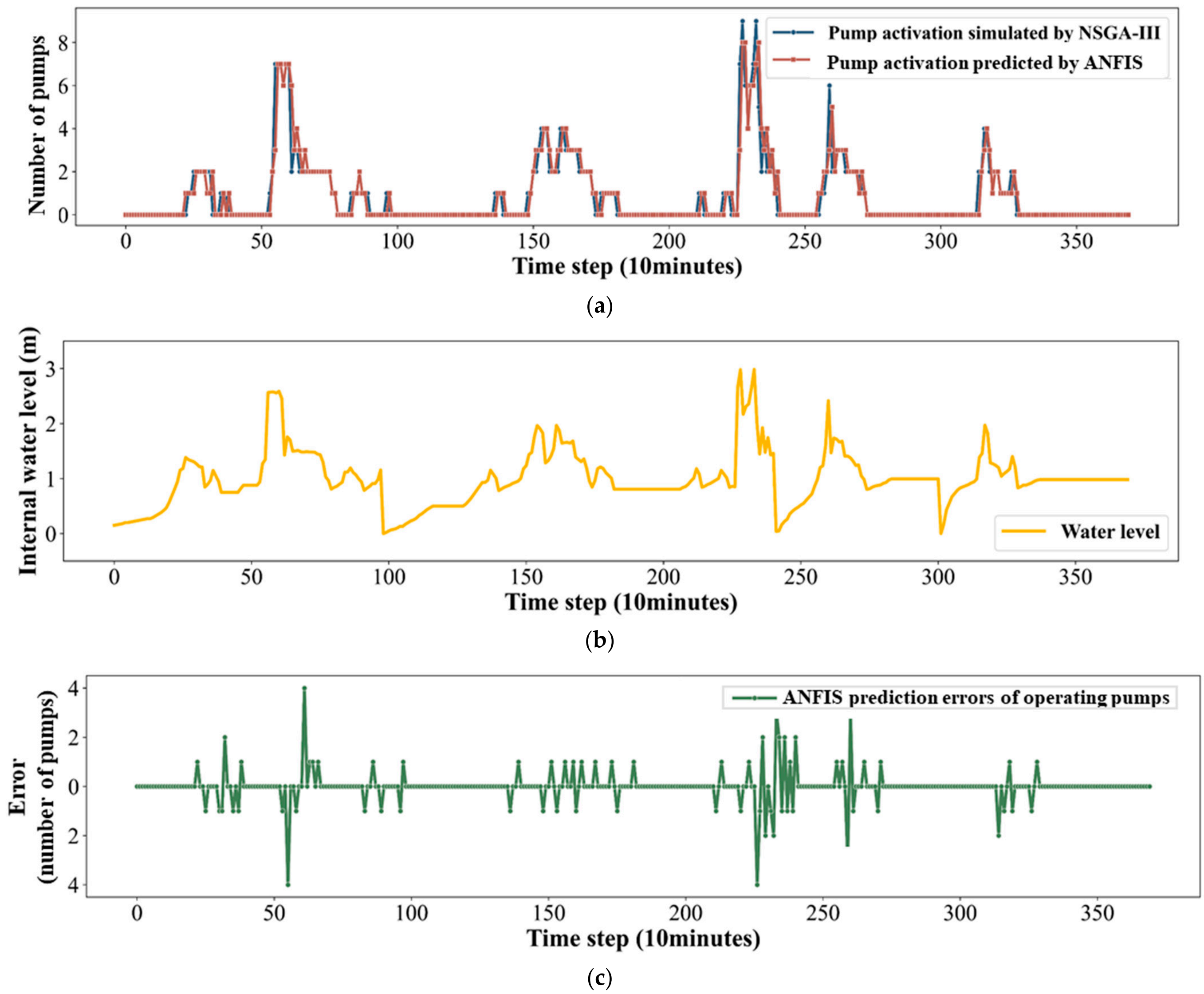

Figure 8. A comparison of the predicted and simulated results for the pump operation models in additional testing phases. The predicted results were generated based on the ANFIS model. The simulation results were generated based on the TOPSIS-selected optimized operational rules obtained from NSGA-III. (**a**) Simulated and predicted operating pumps. (**b**) Internal (forebay) water level. (**c**) ANFIS prediction errors for operating pumps.

3.5.3. Error Distributions and Practical Implications

As shown in Figure 9, the percentage difference between the ANFIS-predicted and NSGA-III-simulated operating pumps was generally within one pump across all stages (training, validation, testing, and additional testing). The most accurate predictions occurred when one to four pumps were activated. However, the model showed a tendency to underestimate the pump activation during medium- to high-demand periods, with occasional errors for up to four pumps.

These results demonstrate the model's capacity to provide accurate short-term forecasts under a range of scenarios, while also identifying areas for improvement in representing high-variability events. Despite its limitations, the ANFIS model significantly enhances automated decision-making, offering valuable early insights for pumping station operators and reinforcing the potential of AI-based systems in real-time flood control management.

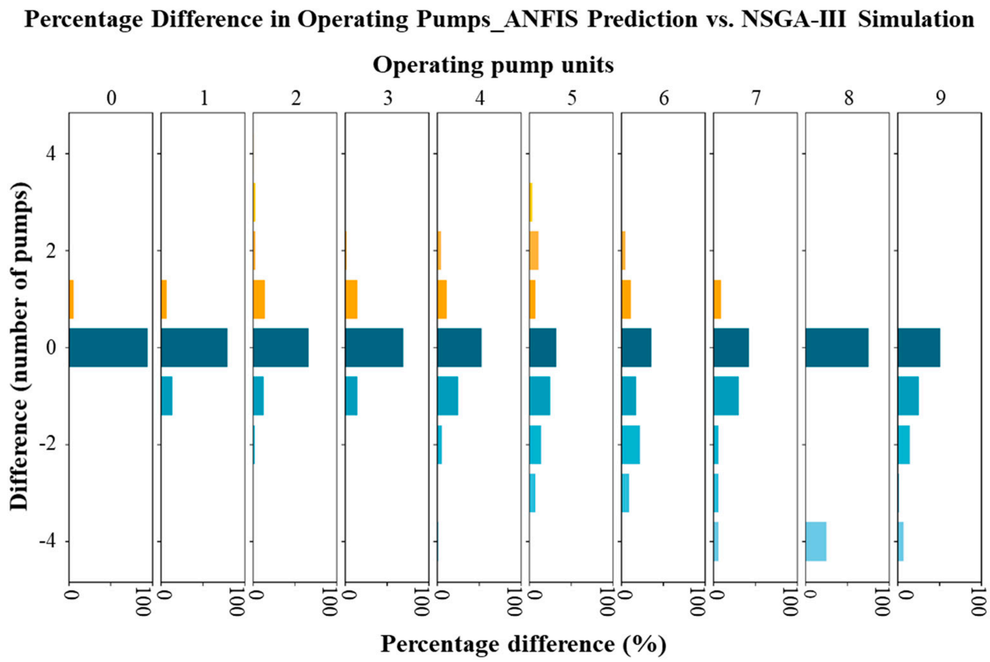

Figure 9. The percentage difference in the operating pumps predicted using the ANFIS and simulated by NSGA-III.

3.6. Discussion

The proposed IFCDSS framework (Figure 2) integrates real-time forecasting, multi-objective optimization, and adaptive control to improve pumping station performance. The CNN-BP model forecasts water levels using historical rainfall and water level data; while pump operations are not direct inputs, their influence is reflected in internal water level patterns, ensuring system responsiveness. NSGA-III optimizes the operational strategies by simulating future system states based on the initial conditions and proposed rules, with the pump switching frequency as a key objective. The ANFIS then uses the optimized outputs and forecasted water levels to predict the pump requirements in real time, enabling adaptive and efficient responses. The integrated use of data-driven forecasting, evolutionary optimization, and real-time control makes the IFCDSS a robust, intelligent solution for urban flood management. It supports autonomous and sustainable operations, aligning with smart city goals and enhancing climate resilience.

It is noted that NSGA-III was employed to optimize the pumping station's operational strategies using historical flood event data. Specifically, the dataset was divided into 24 training events (comprising 2120 data points) and 14 testing events (comprising 659 data points), based on historical inflow and operational records. The training data were used to simulate the system's responses under various operational strategies, incorporating the initial water levels, inflow conditions, and pump operation records to evaluate objective functions and refine the optimization process. Regarding the stationarity of the data, we recognize that urban hydrological systems are inherently subject to long-term non-stationary influences such as land use changes and climate variability. However, for the purposes of this study, we assumed relative short-term stationarity in both the hydrological and infrastructural conditions over the selected study period. This assumption is supported by the observed consistency in the rainfall patterns, inflow characteristics, and operational settings across the selected events.

While the ANFIS model effectively captured the overall operational trends, it exhibited systematic underpredictions during rapid rises in water levels and delayed responses during recession phases—likely due to its limited sensitivity to abrupt system changes. Notably, under conditions of stable water levels or moderate pump activity, the ANFIS model demonstrated an excellent predictive accuracy, reliably estimating the pump requirements and contributing to effective internal water level management.

It is recognized that the pump operation data play a critical role in the optimization phase of the IFCDSS—specifically for the objective function Obj_3, which aims to minimize the pump switching frequency within the NSGA-III optimization process. While these data (i.e., the number of activated pumps) are not used directly as an input in the CNN-BP model for water level forecasting, it strongly influences fluctuations in internal (forebay) water levels, which are included as input features in the forecasting model. Therefore, although CNN-BP does not explicitly use pump operation data, their indirect influence is reflected through the internal water level dynamics.

While this study acknowledges certain limitations—such as the exclusion of gravity drainage—it also offers a deeper assessment of the scalability and broader applicability of the IFCDSS framework. To evaluate its generalizability in future study, the model should be applied to datasets from cities with diverse hydrological, infrastructural, and climatic conditions. Testing under extreme scenarios, such as high-intensity typhoons and compound flooding events, will be crucial to validate the system's robustness and reliability in the face of escalating climate risks.

Further efforts should also aim to enhance the model's resilience to extreme flood conditions and improve the transparency of AI-driven decision-making. Incorporating machine learning techniques to generate high-resolution rainfall forecasts (e.g., at 10 min intervals) may significantly boost the water level prediction accuracy. Moreover, integrating pump operation data directly into the forecasting model could improve its performance, particularly in situations where pumping activity strongly influences internal water levels.

4. Conclusions

As climate change accelerates the occurrence and severity of extreme rainfall events, the demand for intelligent and adaptive flood management solutions has become increasingly critical. This study introduces the Intelligent Flood Control Decision Support System (IFCDSS), an advanced, AI-driven framework developed to comprehensively enhance urban flood resilience. By integrating CNN-BP for accurate real-time water-level forecasting, NSGA-III for effective multi-objective optimization, the TOPSIS for strategic solution selection, and the ANFIS for adaptive pump operations, the IFCDSS significantly advances proactive flood management capabilities.

Successfully applied in Taipei's flood-prone Zhongshan Pumping Station catchment, the IFCDSS demonstrated its capability by delivering accurate forecasts ($R^2 > 0.81$) within five seconds for the subsequent 10 to 30 min. While traditional manual operations narrowly achieved slightly better peak flood reductions due to their singular focus on minimizing flood hazards, the IFCDSS clearly excelled at simultaneously optimizing multiple critical objectives, including flood hazard mitigation, energy efficiency, and operational reliability, thereby highlighting its superior practical value.

The AI-driven techniques underpinning the IFCDSS have effectively transformed urban flood management through efficient processing of complex datasets such as satellite imagery, meteorological inputs, and terrain information. By learning from historical flood patterns and integrating real-time IoT data, the system facilitates rapid forecasting and enables the development of digital twins. Crucially, the adaptive capabilities of the ANFIS automate pumping station operations, dynamically optimizing pump activation decisions and substantially improving operational responsiveness, the effectiveness of flood mitigation, and infrastructure resilience compared to conventional approaches.

The flexible, cloud-based architecture of the IFCDSS allows for scalable deployment and adaptability across diverse urban environments, positioning it as an essential tool for future-oriented, climate-resilient urban infrastructure. This study underscores the transformative potential of integrated AI solutions in protecting communities and infrastructure from intensifying flood risks, advancing sustainable urban development, and providing a reliable blueprint for modern urban flood control management.

Supplementary Materials: The following supporting information can be downloaded at https://www.mdpi.com/article/10.3390/smartcities8030091/s1. Figure S1: A comparison between observed and forecasted sewer, internal and external water levels from the CNN-BP model for the Typhoon Kompasu event; Table S1: Hyperparameter settings of the CNN-BP.

Author Contributions: Conceptualization: L.-C.C. and F.-J.C. Methodology: L.-C.C. and F.-J.C. Software: L.-C.C. and M.-T.Y. Validation: L.-C.C., M.-T.Y., and J.-Y.L. Formal analysis: M.-T.Y. and P.-Y.K. Investigation: M.-T.Y. Resources: M.-T.Y. and J.-Y.L. Data curation: M.-T.Y. Writing—original draft preparation: L.-C.C. and M.-T.Y. Writing—review and editing: F.-J.C. Visualization: L.-C.C. Supervision: F.-J.C. Project administration: F.-J.C. Funding acquisition: L.-C.C. and F.-J.C. All authors have read and agreed to the published version of the manuscript.

Funding: This research was funded by the National Science and Technology Council, Taiwan, grant numbers NSTC 112-2625-M-002-022- and 113-2313-B-002-029-MY3; the Taipei City Government, grant number H-111-99-111084-1; and National Taiwan University, grant number NTU-CC-114L894801.

Data Availability Statement: The data can be made available upon reasonable request to the corresponding author due to restrictions (the project policy).

Acknowledgments: The datasets provided by the Taipei City Government's Hydraulic Engineering Office are acknowledged. The authors also extend their sincere appreciation to the editors and anonymous reviewers for their valuable and constructive feedback, which significantly enhanced the quality and depth of this article.

Conflicts of Interest: The authors declare no conflicts of interest.

References

1. Jato-Espino, D.; Manchado, C.; Roldán-Valcarce, A.; Moscardó, V. ArcUHI: A GIS add-in for automated modelling of the Urban Heat Island effect through machine learning. *Urban Clim.* **2022**, *44*, 101203.
2. Tang, W.; Ye, C.; Zhang, Q.; Li, J.; Ao, F.; Zheng, B.; Luo, Y. Study on the carbon sequestration performance and barrier mechanism of biochar cement-based vertical cutoff walls for phenol pollution in groundwater. *J. Environ. Chem. Eng.* **2024**, *12*, 114560.
3. Webber, J.L.; Fletcher, T.; Farmani, R.; Butler, D.; Melville-Shreeve, P. Moving to a future of smart stormwater management: A review and framework for terminology, research, and future perspectives. *Water Res.* **2022**, *218*, 118409.
4. Almulhim, A.I. Building Urban Resilience Through Smart City Planning: A Systematic Literature Review. *Smart Cities* **2025**, *8*, 22.
5. IPCC. *AR5 Synthesis Report: Climate Change 2014*; Intergovernmental Panel on Climate Change: Geneva, Switzerland, 2014.
6. Alkhatib, M.I.I.; Talei, A.; Chang, T.K.; Pauwels, V.R.N.; Chow, M.F. An Urban Acoustic Rainfall Estimation Technique Using a CNN Inversion Approach for Potential Smart City Applications. *Smart Cities* **2023**, *6*, 3112–3137.
7. Balogun, A.L.; Marks, D.; Sharma, R.; Shekhar, H.; Balmes, C.; Maheng, D.; Arshad, A.; Salehi, P. Assessing the potentials of digitalization as a tool for climate change adaptation and sustainable development in urban centres. *Sustain. Cities Soc.* **2020**, *53*, 101888.
8. Yereseme, A.K.; Surendra, H.J.; Kuntoji, G. Sustainable integrated urban flood management strategies for planning of smart cities: A review. *Sustain. Water Resour. Manag.* **2022**, *8*, 85.
9. Abid, S.K.; Sulaiman, N.; Chan, S.W.; Nazir, U.; Abid, M.; Han, H.; Ariza-Montes, A.; Vega-Muñoz, A. Toward an integrated disaster management approach: How artificial intelligence can boost disaster management. *Sustainability* **2021**, *13*, 12560. [CrossRef]
10. Agboola, O.P.; Tunay, M. Urban resilience in the digital age: The influence of Information-Communication Technology for sustainability. *J. Clean. Prod.* **2023**, *428*, 139304.
11. Allam, Z.; Dhunny, Z.A. On big data, artificial intelligence and smart cities. *Cities* **2019**, *89*, 80–91.
12. Fan, C.; Zhang, C.; Yahja, A.; Mostafavi, A. Disaster City Digital Twin: A vision for integrating artificial and human intelligence for disaster management. *Int. J. Inf. Manag.* **2021**, *56*, 102049.
13. Rentachintala, L.R.N.P.; Reddy, M.M.; Mohapatra, P.K. Urban stormwater management for sustainable and resilient measures and practices: A review. *Water Sci. Technol.* **2022**, *85*, 1120–1140.

14. Suits, K.; Annus, I.; Kändler, N.; Karlsson, T.; Maris, A.V.; Kaseva, A.; Rajarao, G.K. Overview of the (Smart) Stormwater Management around the Baltic Sea. *Water* **2023**, *15*, 1623. [CrossRef]
15. Sweetapple, C.; Webber, J.; Hastings, A.; Melville-Shreeve, P. Realising smarter stormwater management: A review of the barriers and a roadmap for real world application. *Water Res.* **2023**, *244*, 120505. [PubMed]
16. Aboualola, M.; Abualsaud, K.; Khattab, T.; Zorba, N.; Hassanein, H.S. Edge technologies for disaster management: A survey of social media and artificial intelligence integration. *IEEE Access* **2023**, *11*, 73782–73802.
17. Chanchayanon, T.; Chaiprakaikeow, S.; Jotisankasa, A.; Inazumi, S. Optimization of Geothermal Heat Pump Systems for Sustainable Urban Development in Southeast Asia. *Smart Cities* **2024**, *7*, 1390–1413.
18. Zabihi, O.; Siamaki, M.; Gheibi, M.; Akrami, M.; Hajiaghaei-Keshteli, M. A smart sustainable system for flood damage management with the application of artificial intelligence and multi-criteria decision-making computations. *Int. J. Disaster Risk Reduct.* **2023**, *84*, 103470.
19. Razavi-Termeh, S.V.; Pourzangbar, A.; Sadeghi-Niaraki, A.; Franca, M.J.; Choi, S.M. Metaheuristic-driven enhancement of categorical boosting algorithm for flood-prone areas mapping. *Int. J. Appl. Earth Obs. Geoinf.* **2025**, *136*, 104357.
20. Pourzangbar, A.; Oberle, P.; Kron, A.; Franca, M.J. Analysis of the utilization of machine learning to map flood susceptibility. *J. Flood Risk Manag.* **2025**, *18*, e70042.
21. Sun, L.; Xia, J.; She, D.; Ding, W.; Jiang, J.; Liu, B.; Zhao, F. A predictive fuzzy logic and rule-based control approach for practical real-time operation of urban stormwater storage system. *Water Res.* **2024**, *266*, 122437.
22. Pham, B.T.; Luu, C.; Van Phong, T.; Nguyen, H.D.; Van Le, H.; Tran, T.Q.; Prakash, I. Flood risk assessment using hybrid artificial intelligence models integrated with multi-criteria decision analysis in Quang Nam Province, Vietnam. *J. Hydrol.* **2021**, *592*, 125815.
23. Chang, L.C.; Liou, J.Y.; Chang, F.J. Spatial-temporal flood inundation nowcasts by fusing machine learning methods and principal component analysis. *J. Hydrol.* **2022**, *612*, 128086.
24. Huang, P.C.; Lee, K.T. An alternative for predicting real-time water levels of urban drainage systems. *J. Environ. Manag.* **2023**, *347*, 119099.
25. Kao, I.F.; Liou, J.Y.; Lee, M.H.; Chang, F.J. Fusing stacked autoencoder and long short-term memory for regional multistep-ahead flood inundation forecasts. *J. Hydrol.* **2021**, *598*, 126371.
26. Moeini, R.; Nasiri, K.; Hosseini, S.H. Predicting the Water Inflow Into the Dam Reservoir Using the Hybrid Intelligent GP-ANN-NSGA-II Method. *Water Resour. Manag.* **2024**, *38*, 4137–4159.
27. Jalili, A.A.; Najarchi, M.; Shabanlou, S.; Jafarinia, R. Multi-objective optimization of water resources in real time based on integration of NSGA-II and support vector machines. *Environ. Sci. Pollut. Res.* **2023**, *30*, 16464–16475.
28. Harif, S.; Azizyan, G.; Dehghani Darmian, M.; Givehchi, M. Selecting the best location of water quality sensors in water distribution networks by considering the importance of nodes and contaminations using NSGA-III. *Environ. Sci. Pollut. Res.* **2023**, *30*, 53229–53252.
29. Martínez-Comesaña, M.; Eguía-Oller, P.; Martínez-Torres, J.; Febrero-Garrido, L.; Granada-Álvarez, E. Optimisation of thermal comfort and indoor air quality estimations applied to in-use buildings combining NSGA-III and XGBoost. *Sustain. Cities Soc.* **2022**, *80*, 103723.
30. Tang, X.; He, Y.; Qi, P.; Chang, Z.; Jiang, M.; Dai, Z. A new multi-objective optimization model of water resources considering fairness and water shortage risk. *Water* **2021**, *13*, 2648. [CrossRef]
31. Yan, P.; Zhang, Z.; Lei, X.; Hou, Q.; Wang, H. A multi-objective optimal control model of cascade pumping stations considering both cost and safety. *J. Clean. Prod.* **2022**, *345*, 131171.
32. Yang, S.N.; Chang, L.C.; Chang, F.J. AI-based design of urban stormwater detention facilities accounting for carryover storage. *J. Hydrol.* **2019**, *575*, 1111–1122. [CrossRef]
33. Liu, R.; Liu, Y.; Jiao, L.; Wang, L. Multi-objective optimization of reservoir group operation after Inter basin water transfer jointing SWAT model and NSGA-II. *J. Hydrol.* **2025**, *660*, 133431. [CrossRef]
34. Lin, S.S.; Shen, S.L.; Zhang, N.; Zhou, A. Comprehensive environmental impact evaluation for concrete mixing station (CMS) based on improved TOPSIS method. *Sustain. Cities Soc.* **2021**, *69*, 102838. [CrossRef]
35. Lin, S.S.; Zhou, A.; Shen, S.L. Safety assessment of excavation system via TOPSIS-based MCDM modelling in fuzzy environment. *Appl. Soft Comput.* **2023**, *138*, 110206. [CrossRef]
36. Singh, S.; Agrawal, V.; Saxena, K.K.; Mohammed, K.A. Optimization on manufacturing processes at Indian industries using TOPSIS. *Indian J. Eng. Mater. Sci.* **2023**, *30*, 32–44.
37. Zhou, Y.; Liu, Z.; Zhang, B.; Yang, Q. Evaluating water resources carrying capacity of Pearl River Delta by entropy weight-TOPSIS model. *Front. Environ. Sci.* **2022**, *10*, 967775. [CrossRef]
38. Chang, F.J.; Chang, Y.T. Adaptive neuro-fuzzy inference system for prediction of water level in reservoir. *Adv. Water Resour.* **2006**, *29*, 1–10. [CrossRef]

39. Mardani Najafabadi, M.; Mirzaei, A.; Azarm, H.; Nikmehr, S. Managing water supply and demand to achieve economic and environmental objectives: Application of mathematical programming and ANFIS models. *Water Resour. Manag.* **2022**, *36*, 3007–3027. [CrossRef]
40. Wee, G.; Chang, L.C.; Chang, F.J.; Amin, M.Z.M. A flood impact-based forecasting system by fuzzy inference techniques. *J. Hydrol.* **2023**, *625*, 130117. [CrossRef]
41. Zhou, Y.; Guo, S.; Chang, F.J. Explore an evolutionary recurrent ANFIS for modelling multi-step-ahead flood forecasts. *J. Hydrol.* **2019**, *570*, 343–355. [CrossRef]
42. Chang, L.C.; Yang, M.T.; Chang, F.J. Flood resilience through hybrid deep learning: Advanced forecasting for Taipei's urban drainage system. *J. Environ. Manag.* **2025**, *379*, 124835. [CrossRef] [PubMed]
43. Deb, K.; Agrawal, S.; Pratap, A.; Meyarivan, T. A fast elitist non-dominated sorting genetic algorithm for multi-objective optimization: NSGA-II. In *Parallel Problem Solving from Nature PPSN VI*; Springer: Berlin/Heidelberg, Germany, 2000; Volume 6, pp. 849–858.
44. Deb, K.; Jain, H. An evolutionary many-objective optimization algorithm using reference-point-based nondominated sorting approach, part I: Solving problems with box constraints. *IEEE Trans. Evol. Comput.* **2013**, *18*, 577–601. [CrossRef]
45. Bahrami, N.; Nikoo, M.R.; Al-Rawas, G.; Al-Wardy, M.; Gandomi, A.H. Reservoir optimal operation with an integrated approach for managing floods and droughts using NSGA-III and prospect behavioral theory. *J. Hydrol.* **2022**, *610*, 127961. [CrossRef]
46. Cao, X.; Wen, Z.; Xu, J.; De Clercq, D.; Wang, Y.; Tao, Y. Many-objective optimization of technology implementation in the industrial symbiosis system based on a modified NSGA-III. *J. Clean. Prod.* **2020**, *245*, 118810. [CrossRef]
47. Lyu, J.; Jiang, Y.; Xu, C.; Liu, Y.; Su, Z.; Liu, J.; He, J. Multi-objective winter wheat irrigation strategies optimization based on coupling AquaCrop-OSPy and NSGA-III. *Sci. Total Environ.* **2022**, *843*, 157104. [CrossRef]
48. Wang, M.; Zheng, S.; Sweetapple, C. A framework for comparing multi-objective optimization approaches for a stormwater drainage pumping system. *Water* **2022**, *14*, 1248. [CrossRef]
49. Wang, Y.; Chen, C.; Tao, Y.; Wen, Z.; Chen, B.; Zhang, H. A many-objective optimization of industrial environmental management using NSGA-III. *Appl. Energy* **2019**, *242*, 46–56. [CrossRef]
50. Hwang, C.L.; Yoon, K. Methods for multiple attribute decision making. In *Multiple Attribute Decision Making*; Springer: Berlin/Heidelberg, Germany, 1981; pp. 58–191.
51. Ning, Z.; Zhou, Y.; He, J.; Tang, C.; Xu, C.Y.; Chang, F.J. Balancing water, power, and carbon: A synergistic optimization framework for mega cascade reservoir operations. *Renew. Energy* **2025**, *243*, 122567. [CrossRef]
52. Zhou, Y.; Chang, F.J.; Chang, L.C.; Herricks, E. Elevating urban sustainability: An intelligent framework for optimizing water-energy-food nexus synergies in metabolic landscapes. *Appl. Energy* **2024**, *360*, 122849. [CrossRef]
53. Li, S.; Zhu, D.; Lin, F.; Xia, J.; Zhou, Y.; Chang, F.J.; Xu, C.Y. Unlocking synergies of drawdown operation: Multi-objective optimization of reservoir emergency storage capacity. *J. Environ. Manag.* **2024**, *368*, 122148. [CrossRef]
54. Jang, J.S. ANFIS: Adaptive-network-based fuzzy inference system. *IEEE Trans. Syst. Man Cybern.* **1993**, *23*, 665. [CrossRef]